The Iraqi Journal For Mechanical And Material Engineering, Vol.9, No.2, 2009

Detection of Crack in a Simple Unswept Wing Using Free Vibration Analysis

Hatem. H. Obeid, Nawras Haidar Mostafa, Salwan Obeed Waheed, and Sattar Hantosh.
College of Engineering-Babylon University, Iraq

ABSTRACT:

The present research is concerned with an investigation of the vibration characteristics of a cracked wing structure. Finite element method has been used to formulate the free vibration analysis. Ansys v9.0 program as a mathematical tool was used in implementation the analysis and extract the results. Effect of several parameters such as (effect of crack ratio, crack location, and crack inclination angle) on the natural frequencies and mode shapes were studied. The results indicate that the natural frequencies are affected in the presence of a crack; but it doesn't give an indication to the crack location. While, using mode shape is a powerful tool to detect the crack and its magnitude along the wing's length. The crack inclination angle is investigated to show its effect on the crack identification where relatively little error may appear if crack angle wasn't normal to the wing axis. Also the presence of the crack may cause to transform and exchange the modes between each other depending on the crack location and its magnitude.

الكشف عن الشق لجناح بسيط غير مرتد بأستخدام تحليل الأهتزاز الحر

الخلاصة :

في هذا البحث، تم دراسة خصائص الاهتزاز لتركيب جناح طائرة يحيوي على شق. أستخدمت طريقة العناصر المحددة لصياغة وتحليل الاهتزاز الحر. تم تنفيذ البحث واستخراج النتائج بأستخدام (Ansys v9.0) كوسيلة حل رياضية. تمت دراسة بعض العناصر المؤثرة (مثل نسبة الشق، موقع الشق, و وزاوية ميلان الشق) ومدى تأثيرها على التردد الطبيعي والشكل النمطي (Mode shape) للجناح.أ ظهرت النتائج بأن قيم التردد الطبيعي تتأثر بشكل كبير عند وجود الشق ولكن لا يعطي اية انطباعات عن موقع الشق وقيمته. بينما نتائج الشكل النمطي تمثل وسيلة ممتازة للكشف عن موقع و قيمة الشق على طول الجناح. كما تم دراسة تأثير ميلان زاوية الشق على تحديد موقع الشق حيث أظهرت النتائج وجود خطأ قليل نسبياً في حالة كون زاوية الميلان غير عمودية على محور الجناح. أضافة الى ذلك، أن وجود الشق قد يؤدي الى تحول و أنتقال الأشكال النمطيه فيما بينها وذلك بالأعتماد على موقع ومقدار الشق.

dynamics of a structure is largely depends on the way of various damages undertaken. Since damage (e.g., crack, corrosion, creep) in a structure usually changes the mass, stiffness and/or damping distribution of the structure either locally or globally, vibration characteristics of the structure may be changed so that evaluation of vibration responses may be used to detect the damage. The importance and summary on previous research can be found in several survey papers, for instance the one by Doebling *et al*. (1998).

Since the dynamical motion of a real wing structure is difficult by self to understand deeply. Therefore an attention is focused here on the theoretical study of simple cracked wing (not real) made of aluminum material vibrating in the coupled bending and torsional modes. Additional boundary conditions at the crack location can be established such that the wing can be replaced with two intact wings connected at the crack location or by subtract the crack volume from the whole wing volume. The changes in natural frequencies and mode shapes with respect to the crack location, crack ratio, and crack inclination angle were plotted such that the crack is detected in the wing using free vibration analysis.

2- Crack Detection:

2-1-Based on Changes in Natural Frequencies:

While natural frequencies are relatively easier and more accurately measured than other modal parameters, solving an inverse problem for crack detection based only on changes in natural frequencies is not so easy, considering this fact that natural frequency has a global nature while damage in most cases is a local phenomenon. However, if the crack is the most possible failure mode and no other form of damage exists, detecting the crack by natural frequencies is possible, even with the presence of measurement errors. Various structures have been targeted directly for real applications in civil infrastructure, aeronautical and astronautic systems, ground vehicles, offshore platforms and underground pipelines.

Early systematic investigation on damage detection by changes in natural frequencies may be attributed to Adams *et al*. (1978) and Cawley and Adams (1979). Under the premise that the change in stiffness is independent of frequency, the ratio of frequency changes in two modes is only a function of the damage location. Experiments were carried out on an aluminum plate with damage in the form of a rectangular hole. Stubbs and Osegueda (1990a, 1990b) developed a sensitivity approach for damage detection from changes in natural frequencies that is based on the so-called Cawley-Adams criterion. Salawu (1997) provided a good review on damage detection by changes in natural frequencies. Although it might not be so reliable using natural frequency changes alone for damage identification in some infrastructures such as prestressed concrete structures as indicated in the paper, many strategies and algorithms were developed to further explore the advantages of natural frequencies.

2-2- Mode Shapes/Curvatures:

Mode shapes are known as the spatial description of the amplitude at each resonance frequency. The modal assurance criterion (MAC) and related variations were developed in last two decades as a quality assurance indicator to explore the spatial

modal information in the area of experimental and analytical structural dynamics (Allemang, 2002). West (1984) proposed possibly the first systematic investigation on damage detection by using MAC as the statistical indicator correlating mode shapes of the damaged and undamaged structure without the use of a prior finite element model. Another widely used criterion in damage detection is coordinate modal assurance criterion (COMAC) that identifies the coordinates where two sets of mode shapes do not agree (Lieven and Ewins, 1988). Examples with a focus primarily on MAC and COMAC include Yuen (1985), Natke and Cempel (1997) and Marwala and Hunt (2000). Furthermore, Ratcliffe (1997) proposed a method for damage detection based solely on mode shapes. The location of damage can be identified from the finite difference approximation of a Laplacian operator to the mode shapes. Khan *et al.* (1999) used a continuously scanning laser Doppler vibrometer to monitor the discontinuities in mode shapes for detecting cracks and slots. Shi *et al*. (2000) formulated the MDLAC with incomplete mode shapes instead of natural frequencies for damage detection.

As an alternative in using mode shapes, curvature mode shapes were proposed and considered more sensitive to damage than the displacement mode shapes (Pandey *et al*., 1991). Lew *et al*. (1997) compared the method by curvature mode shapes with two other modal based methods and found it is reliable for beam-type structures but not suitable for truss-type structures. Amaravadi *et al*. (2001) obtained the curvature mode shapes by differentiating mode shapes twice, and then combined a wavelet map with them to improve the sensitivity and accuracy for locating damage in a lattice structure and a cantilever beam.

2-3-Based on Damping:

Although the estimation of damping matrix (mass and stiffness matrices as well) by frequency response functions may be used in the detection of the damage in the structure. Frequency response functions (FRF) depict in frequency domain the input/output relationship for a system, and are extensively used in structural dynamics and system identification to extract resonance frequencies, estimate mode shapes and damping coefficients, and verify matrices of mass, stiffness and damping. Many damage detection methods based on evaluation of modal parameters aforementioned rely on some FRF data, directly or indirectly.

Changes in damping, however, may have the ability to detect damage to which conventional methods based on changes in natural frequencies and mode shapes are not sensitive. Modena *et al*. (1999) showed that visually undetectable cracks cause negligible changes in natural frequencies, but a considerable increase in damping that can be used to locate the cracking.

2-4-Time Domain Features:

Modal parameters and FRF data usually involve data reduction and feature extraction during the transform of recorded data in time domain to features in frequency domain. The process may cause loss of important information related to damage dynamics; this disadvantage could be avoided by directly using time response data for damage detection. Another advantage of using time domain features is that

non-linearity responses raised by damage in a structure could be preserved further facilitating diagnostics.

Cattarius and Inman (1997) proposed a time-domain approach by taking the advantage of beating phenomenon to detect small damage that many be unnoticeable in natural frequency changes. Carneiro and Inman (2000) investigated the detection of a surface crack on a Timoshenko beam in time domain with the aid of an analytical model developed by the authors. A bilinear model of a closing crack is also considered. While the minimum rank perturbation theory (MRPT) has been extensively investigated in frequency domain by Zimmerman and his co-workers (1994) for damage detection.

2-5-Based on Wave Propagation:

As one class of the widely used approaches, wave propagation methods adopt a transmitter and a receiver to send a diagnostic stress wave along the structure and measure the changes in the received signal due to the presence of damage in the structure. This approach is a natural extension is very effective in detecting damage in the form of geometrical discontinuities. In a paper by Van Den Abeele *et al*. (2001) micro-scale damage in a micro-inhomogeneous material were detected by means of nonlinear elastic wave spectroscopy. It is shown that distortion in acoustic and ultrasonic waves with nonlinear features can be used to detect cracks and flaws more reliably than linear acoustical methods (measures of wave speed and dissipation).

3. Finite Element Discritization

3.1. General.

At present, the finite element method is the most powerful numerical technique, which offers approximate solution to realistic types of structures such as wings. In the present study, the 20-node structural 3-dimensional solid element is used for discritization of the wing model

3.2 Element Parameters.

Solid186 is used for the 3-D modeling of solid structure. The element is defined by 20 nodes having three degrees of freedom per node: translations in the nodal x, y, and z directions. SOLID186 may have any spatial orientation. The coordinate system for this element is shown in Figure (1) (Ansys Element Manual, 2004).

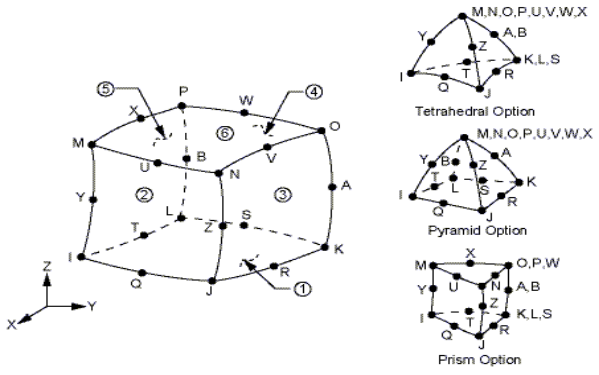

Fig(1): Element geometry.

3.3. Wing Geometry and Mesh Generation.

Figure (2) shows the proposed model (wing), all dimensions of the wing are listed in Table 1 below. The wing was discretized using solid element (solid186). **ANSYS 9.0** finite element program was used as a mathematical tool in the analysis of this model. Where, Figure (3) shows the finite element representation of the wing structure. It must be noted that, the number of the elements at the crack location must be enough in its number to give concentrated results of high accuracy; due to the dramatic changes that occurs at regions of the crack.

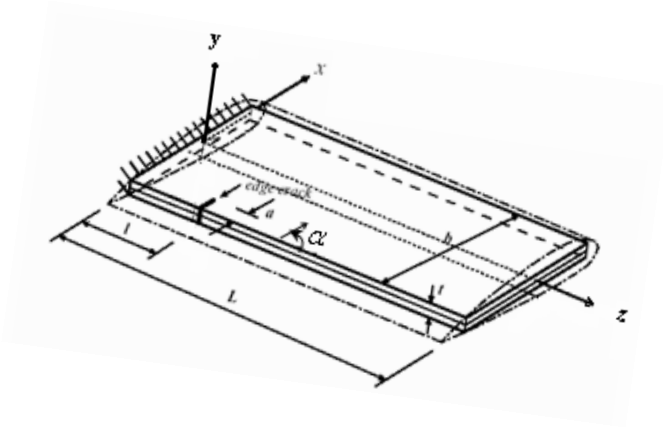

Fig (2): Wing configuration.

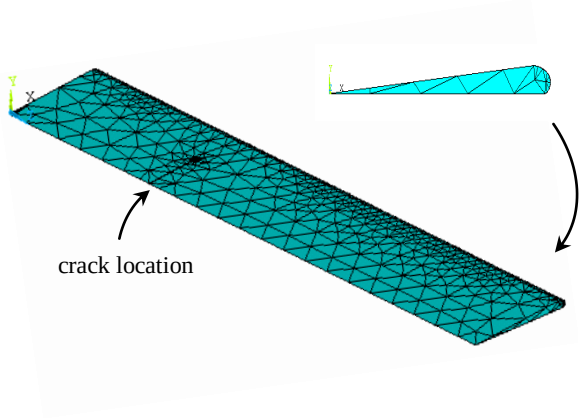

Fig (3): Mesh generation of the wing model.

Table 1 : Proposed dimensions of the wing.

wing length (L)	wing width (b)	maximum wing height(t)	crack location (*l*)	crack width (*a*)	crack inclination angle (α)
100cm	20cm	1.5 cm	variable	variable	variable

3.4. Finite element formulation

The basic concept of the finite elements method is to discretize the continuum into arbitrary numbers of small elements connected together at their common nodes. The stress–strain relations in coordinates aligned with principal material directions are given by:

$$\{\sigma\}=[E]\{\varepsilon\} \qquad \textit{...(1)}$$

For a finite element (**e**), of the discrete model, the displacement vector at any point is:

$$\{u\}^e=[N]\{a\}^e \qquad \textit{...(2)}$$

Where **[N]** is a matrix containing the interpolation functions which relate the element displacement **{u}^{e}** to the nodal displacements **{a}^{e}**. By differentiation of the displacements, the corresponding strains **{ ε }^{e}** are obtained such that:

$$\{\varepsilon\}^e = [A]\{u\}^e \qquad \textbf{…(3)}$$

Where **[A]** is the differential operators matrix.
The substitution of Equation (2) into Equation (3) yields:

$$\{\varepsilon\}^e = [A][N]\{a\}^e \qquad \textbf{…(4)}$$

or

$$\{\varepsilon\}^e = [B]\{a\}^e \qquad \textbf{…(5)}$$

Also, the total solution domain is discretized into a number of elements **(NE)** [sub–domain] such that:

$$\pi(a) = \sum_{e=1}^{NE} \pi^e(a) \qquad \textbf{…(6)}$$

Where π and π^e are the potential energy of the total solution domain and the sub–domain, respectively. The potential energy for an element, **e**, can be expressed in terms of the internal strain energy, **SE**, and external work done, **WF**, such that:

$$\pi^e(a) = SE - WF \qquad \textbf{…(7)}$$

in which (**a)** is the vector of nodal degrees of freedom of an element.
The internal strain energy of an elastic body is given by:

$$SE = \frac{1}{2}\int_A \varepsilon^T \bar{\sigma}\ dA \qquad \textbf{…(8)}$$

then:

$$SE = \frac{1}{2}\{a\}^{eT}\int_A [B]^T [E][B]\ dA\ \{a\} \qquad \textbf{…(9)}$$

The external work done by uniformly distributed load is given by:

$$W_f = \int_A \{a\}\lfloor P \rfloor\ dA \qquad \textbf{…(10)}$$

But, the displacement vector **{a}** can also be defined as:

$$\{a\} = [N]\{a\}^e \qquad \textbf{…(11)}$$

Also

$$W_f = \int_A \{a\}^{eT}[N]^T \lfloor P \rfloor dA \qquad \textbf{…(12)}$$

$$\pi^e(a) = \frac{1}{2}\{a\}^{eT}\int_A [B]^T [E][B]\ dA\ \{a\}^e - \int_A \{a\}^{eT}[N]^T \lfloor P \rfloor\ dA \qquad \textbf{…(13)}$$

To obtain the Equilibrium State of the plate element, the potential energy must be minimized with respect to nodal displacements as follows:

$$\{\frac{\partial \pi}{\partial a^e}\} = \{0\} \qquad \textbf{…(14)}$$

By substitution of Equation (13) in Equation (14) and carrying out the partial differentiation, then:

$$\{\frac{\partial \pi}{\partial a^e}\} = \int_A [\mathrm{B}]^T [\mathrm{E}][\mathrm{B}]\, dA\ \{a\}^e - \int_A [N]^{\mathrm{T}} \lfloor \mathrm{P} \rfloor\, \mathrm{dA} = \{0\} \qquad \textbf{…(15)}$$

or

$$[k]^e \{a\}^e - [F]^e = \{0\} \qquad \textbf{…(16)}$$

where,

$$[k]^e = \int_A [\mathrm{B}]^T [\mathrm{E}][\mathrm{B}]\, dA = \int_{-1}^{1}\int_{-1}^{1} [\mathrm{B}]^T [\mathrm{E}][\mathrm{B}] |J|\, d\xi\, d\eta \qquad \textbf{…(17)}$$

$$[F]^e = \int_A [N]^T \lfloor P \rfloor\, dA = \int_{-1}^{1}\int_{-1}^{1} [N]^T \lfloor P \rfloor |J|\, d\xi\, d\eta \qquad \textbf{…(18)}$$

in which,
$[K]^e$: is the element stiffness matrix,
$[F]^e$: is the element external applied force vector,
J : is the determinant of the **Jacobian** matrix.
In general, it is not possible to evaluate the element stiffness matrix explicitly. Thus, numerical integration has to be used based on **Gauss– quadrature** rules, and the selective integration (Zienkiewicz *et al* ,2000).

3.5. Formulation of element mass matrix:

When the shape functions used for the derivation of the mass matrix are identical to those used in formulating the element stiffness matrix; matrix **[M]** is called the consistent mass matrix.
To derive the consistent mass matrix, one can consider the kinetic energy of the total solution domain discretized into number of elements **(NE**) such that:

$$TI(\dot{a}) = \sum_{e=1}^{NE} TI^e(\dot{a}) \qquad \textbf{…(19)}$$

where **TI** and $\mathbf{TI^e}$ are the kinetic energy of the total solution domain and the sub–domain respectively. The kinetic energy of the element (**e**) can be expressed as follows:

$$TI^e = \frac{1}{2}\int_A \{\dot{a}\}^T [m]\{\dot{a}\} dA \qquad \textbf{…(20)}$$

The velocity vector within an element is discretized such that:

$$\{\dot{a}\} = \sum_{i=1}^{NN} N_i \{\dot{a}_i\} \quad \text{NN (number of nodes)} \qquad \textbf{…(21)}$$

By substituting Equation (21) into Equation (20), and rearrange it into matrix form:

$$TI^e = \frac{1}{2}\{\dot{a}\}^T \int_A [N]^T [m][N] dA \{\dot{a}\} = \frac{1}{2}\{\dot{a}\}^T [M]^e \{\dot{a}\} \quad \textbf{…(22)}$$

thus,

$$[M]^e = \int_A [N]^T [m][N] dA = \int_{-1}^{1}\int_{-1}^{1} [N]^T [m][N] |J| \, d\xi \, d\eta \quad \textbf{…(23)}$$

Where

$[N] = [N_1, N_2, N_3 \ldots N_{nn}]$ **…(24)**

3.6. Modal Analysis:

In the dynamic analysis, the natural frequency, ω, of the vibration is important to give an idea about the oscillation of the system with time, and to determine the natural period (T) of the vibration which represents the time for which the vibration repeats itself, as:

$T = 2\pi/\omega$ **…(25)**

To determine the natural frequencies of a structure, a free vibration

$$[M]\{\ddot{X}\} + [K]\{X\} = 0 \quad \textbf{…(26)}$$

Assuming harmonic motion which yields to:

$$([K] - \omega_i^2 [M])\{\phi_i\}\{\phi_i\}^T = 0 \quad \textbf{…(27)}$$

Equation (27) has the form of the algebraic eigenvalue problem ($\mathbf{K\phi=\lambda M\phi}$). From the theory of homogeneous equations, nontrivial solutions exist only if the determinant of the coefficient matrix is equal to zero. Thus:

$$\left|[K] - \omega_i^2 [M]\right| = 0 \quad \textbf{…(28)}$$

Expansion of the determinant yields a polynomial of order **n** called characteristic equation. The **n** roots of this polynomial **(ω_i^2)** are the characteristic values or the eigenvalues.

3.7. Results and Discussion:

3.7.1 Natural Frequency :

Figure (4) presents the mode shapes and corresponding natural frequencies for the wing structure without crack. As shown, the first mode shape present the minor bending mode in x-y plane of natural frequency equal to (9.1899Hz), the second present the major bending mode in x-y plane of natural frequency (57.035 Hz). Pure torsion is address of the third mode of natural frequency (109.3 Hz). The fourth mode is purely bending in x-z plane of (131.02 Hz). At last, the fifth mode is complex bending in x-y plane of (157.966 Hz).

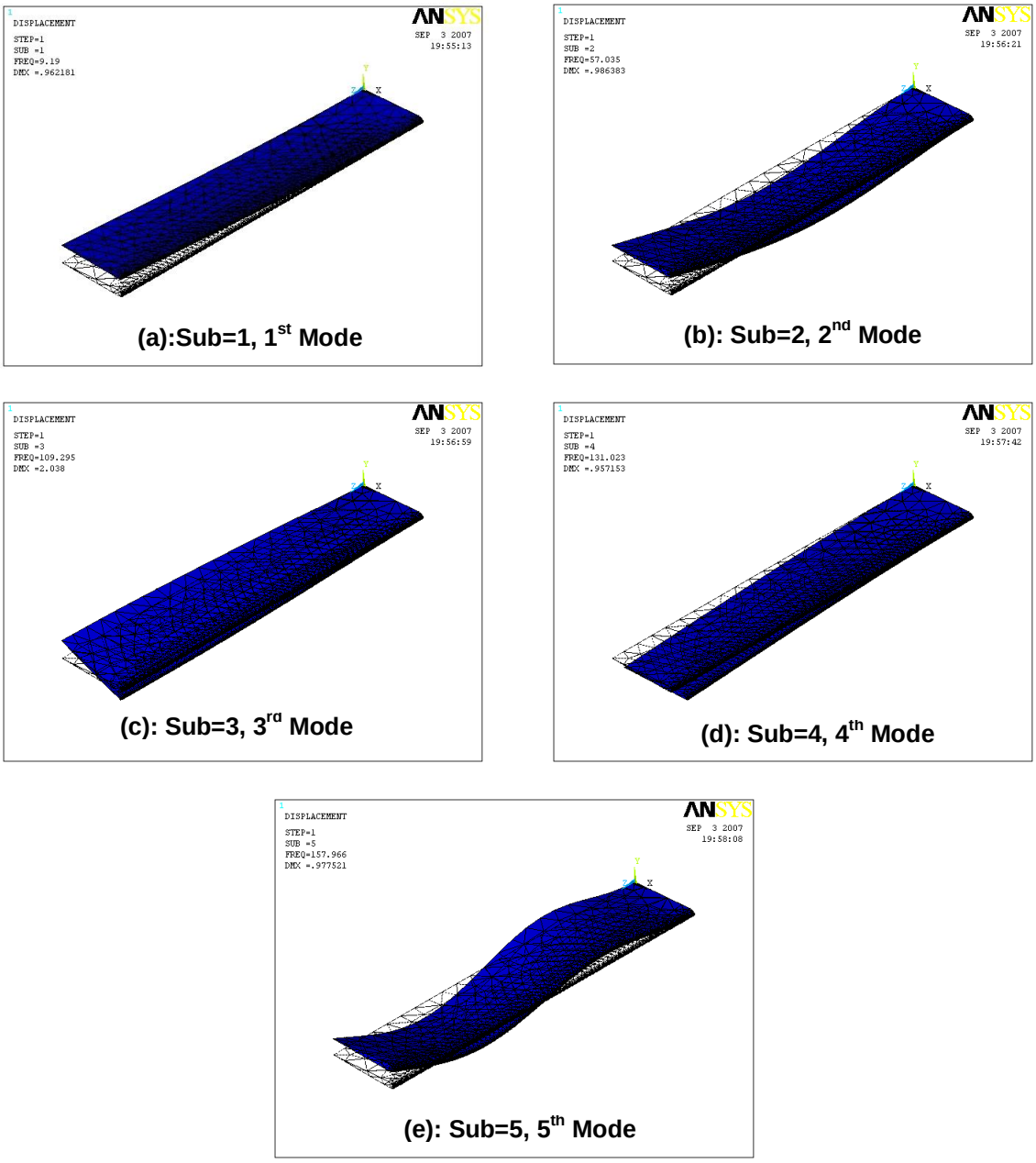

Fig (4): Mode shapes of wing without crack.

Table 2 list the natural frequencies of a cracked wing with different crack ratios which started from 0.1 to 0.9 at a dimensionless crack location (**l/L)** equal to **0.3**. Table 3 shows the change in the natural frequencies with different crack locations using crack ratio **(a/b)** equal to **0.5**.

Table (2):Natural frequency at different crack ratios (η=a/b), ζ =l/L =0.3

modes	η=0.1	η=0.2	η=0.3	η=0.4	η=0.5	η=0.6	η=0.7	η=0.8	η=0.9
first	9.186	9.184	9.184	9.179	9.165	9.141	9.081	8.965	8.636
second	57.013	56.979	56.949	56.939	56.901	56.839	56.64	56.28	32.137

third	109.232	108.904	109.096	109.01	108.625	100.7	84.293	62.063	55.385
fourth	130.783	129.557	126.124	120.675	112.494	108.28	107.158	104.799	98.783
fifth	157.648	157.059	157.191	157.104	156.89	156.33	155.022	152.831	147.706

Table (3): Natural frequency at different crack location (ζ=l/L), η=a/b=0.5

modes	**ζ =0.1**	**ζ =0.2**	**ζ =0.3**	**ζ =0.4**	**ζ =0.5**	**ζ =0.6**	**ζ =0.7**	**ζ =0.8**	**ζ =0.9**
first	9.132	9.158	9.165	9.173	9.178	9.182	9.183	9.184	9.189
second	56.749	56.938	56.897	56.817	56.766	56.773	56.843	56.883	56.96
third	99.48	105.704	108.62	108.84	108.71	108.83	108.72	108.795	109.19
fourth	107.96	108.962	112.47	118.64	123.77	127.49	129.71	130.701	131.01
fifth	156.55	157.21	156.87	156.71	156.72	156.65	156.65	156.597	157.14

It was noted that the natural frequency in the case of wing without crack has a larger values than tables (2, 3) because the presence of the crack have a significant effect on the stiffness (local flexibility) of the structure. In other words, the crack reduces the number of connected element points which reduce the number of the doubled point of the stiffness matrix, thereby reduce the stiffness of the element. As a result, a decreasing in the stiffness will reduce the corresponding natural frequency based on the direct relationship between them. As shown in table (2), it is noted that for the case of constant crack location, changes in natural frequency depend on the changes in the crack length which is surely due to the changing of the overall stiffness of the wing at each crack length.

It was supposed that for each mode, the value of natural frequency decreases gradually with increasing in the crack length (due to the increasing in the unconnected point). This agrees with first and fifth mode shapes and some what in the second mode shape, where dramatic changes happen at crack ratio equal to 0.9, but don't agree with the third mode shape in which the natural frequency decreases dramatically with the increase of the crack ratio that started form 0.5.

In other words, mode transform or mode exchange effect which mean that there are transformations and coupling between the modes; as example at **η=0.9** the second mode (bending in x-y plane) becomes bending mode in the x-z plane as depicted in Figure (5). While the fourth mode (bending in x-z plane) is transformed to become torsion mode after **η=0.5** and vice versa as shown in Figure (6). As well as, it is very clear that the fourth mode (bending in x-z plane) is more sensitive to the crack length than the other modes, because this vibrating mode tends to open the crack.

Table (3) presents the changes in the natural frequency at different crack locations and constant crack ratio. Like Table (2), there are interactions and transformation between the mode shapes. As example, the value of the natural frequency in the fourth mode starts at **ζ=0.1** with a closed value of the third mode at **ζ=0.3** which is the same problem that presence of the mode interactions. The alternative decreasing and increasing in the natural frequency makes the frequency method ineffective in the study of the effect of the crack location on the structure response. On the other hand, in the tables mentioned above, the changes in the natural frequencies are small compared with the big changes in crack ratio and its location, respectively. Tables (2) and (3) were also graphed in normalized form to explain and study the information clearly.

Figure (7), shows that the changes of the normalized natural frequency (the natural frequency with crack divided by the natural frequency without crack) of the first and

fifth modes was very small as compared to the second, third, and fourth modes. The fourth mod was affected at crack ratio started from 0.2 in which the change is smaller than that corresponding to the third and second modes in which the changing is started from crack ratio of 0.5 and 0.8 respectively.

In Figure (8) which presents the relation between the normalized natural frequency and crack location. The changes in the natural frequency in the first, second, and fifth modes were simple and smaller than the corresponding in the third and fourth modes. The maximum effect in the natural frequency occurs in the fourth mode due to the reduction in the stiffness in the horizontal plane that is largely affected by crack presence.

It is important to refer that the changing in the natural frequency due to the change in the crack location and crack ratio doesn't give any useful information about the crack presence, location, and its length. Thus, it is not recommended to depend on the natural frequency changes to test the cracked structure because there information is not valuable. This result agreed with (Wang, K.2004) who reminded that "As the global nature of a structure, natural frequencies may not be sensitive to the local incipient damage. Where some situations such as damage detection on bridges and buildings, changes in environmental conditions (e.g., climate changes) even in a single day could affect natural frequencies more than the possible damage by changing mass and stiffness of the structure".

Figure (9) presents the effect of the crack inclination angle on the natural frequency. It was noted that the changes in natural frequency on the first mode is less than that corresponding of the second, third, and fifth, respectively. But the fourth mode was largely affected with the inclination angle. It is important to refer that the maximum effect occurs at an inclination angle of 90˚ (the crack is normal on the wing axis).

3.7.2 Mode Shapes

3.7.2.1 Line of crack perpendicular on the wing axis.

Figure (10) presents the torsional mode shapes at different crack ratios in the wing. At first glance, it is noted that the crack location (**ζ=0.3**) can be recognized clearly that represented by the vertical line in each mode (discontinuity in mode shape). The length of the vertical line is direct proportional with the crack ratio (an increasing in the crack ratio causes an increasing in the length of the vertical line). Figure (11) presents the bending mode shapes with different crack ratios in which the crack ratio was not clearly affect the dynamic general behavior.

Figure (12) presents the torsional mode shape at different crack locations with constant crack ratio **η=0.5**. It is important to note that there was a sudden jump in each crack location (the vertical line). This jump is largest when the crack location is closest to the root of the wing and decreases gradually when it converged to the wing's tip (converse proportional). The main reason is that the maximum torsional moment in the wing structure occurs at a distance between (0.1- 0.15) from the wing length (highly stressed regions) and decreasing after that (Waheed. S. O, 2006). The jump in the torsional mode is more obvious than the bending mode as depicted in figures (12, 13). However, the deflected shape and its jump at each crack location may still valuable for

detecting the crack location and its length when both bending and torsional modes are taken into consideration.

3.7.2.2 Inclined crack with angle α

Figures (14, 15) presented the torsional and bending mode shapes at different crack inclination angles. The crack ratio and crack length are constants of 0.5. The general behaviors in the figures are the same as in case of perpendicular crack. It was noted that the two modes doesn't largely affected by the changing in the inclination angle. Although that the value of crack location of 0.5 (the discontinuity must appear at this location exactly), there is little shifting of the discontinuity closest to the crack. Anyway this is not a great problem but it may mislead the observer to detect the crack exactlly.

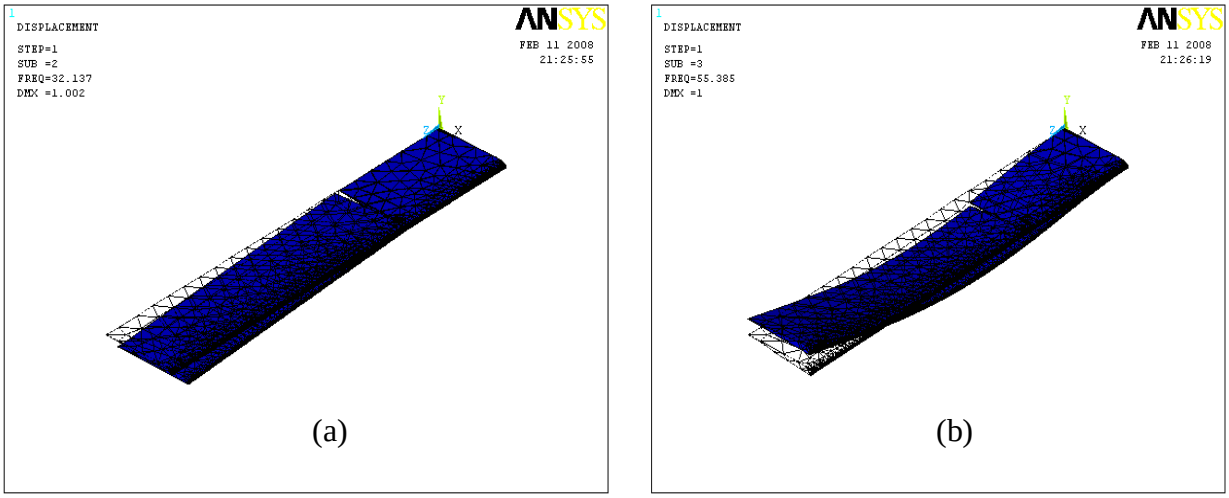

Fig (5): Transforms between modes at (η=0.9), ζ =l/L =0.3
(a) The fourth mode to the second ,(b) second to the third.

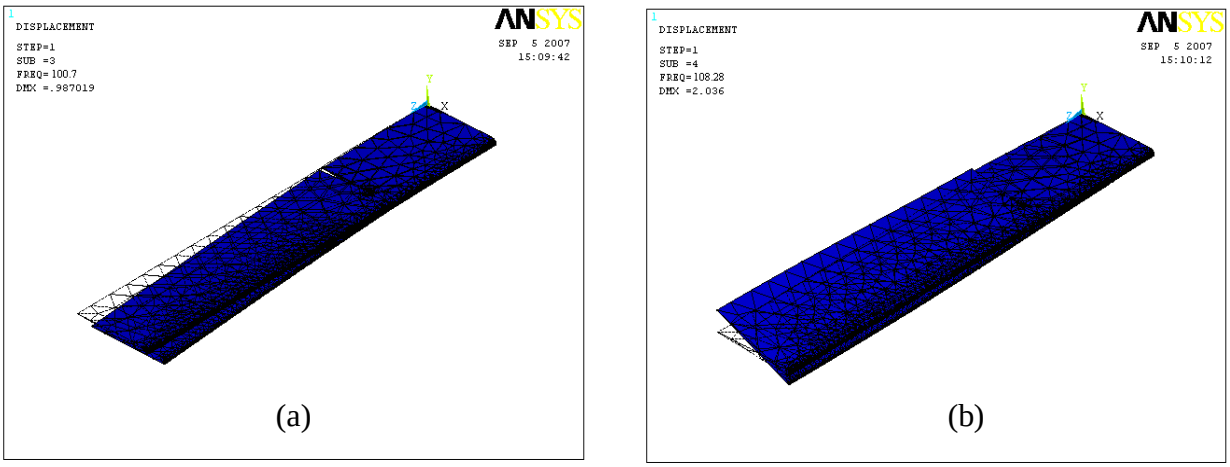

Fig (6): Transforms between modes at (η=0.6), ζ =l/L =0.3
(a) The fourth mode to the third ,(b) the third to the fourth.

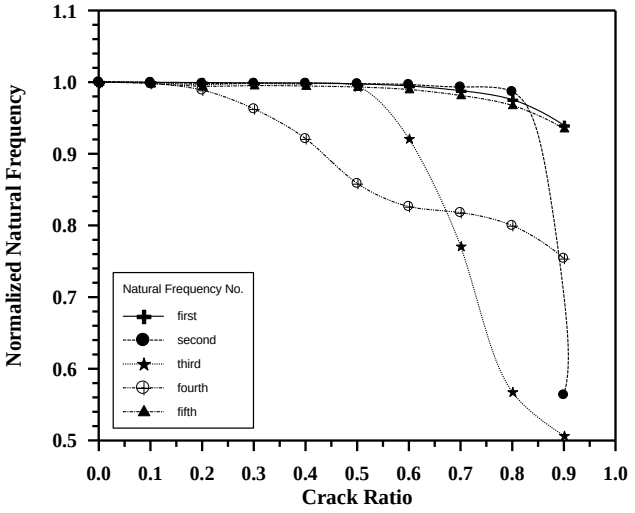

Fig (7): Normalized natural frequency at different crack ratios

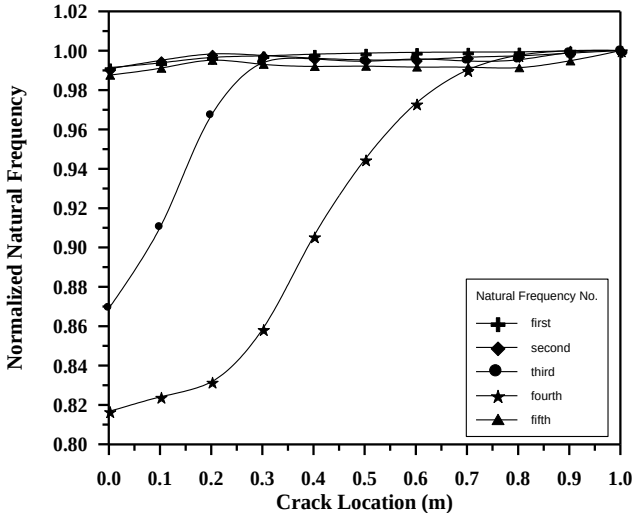

Fig (8): Normalized natural frequency at different crack locations

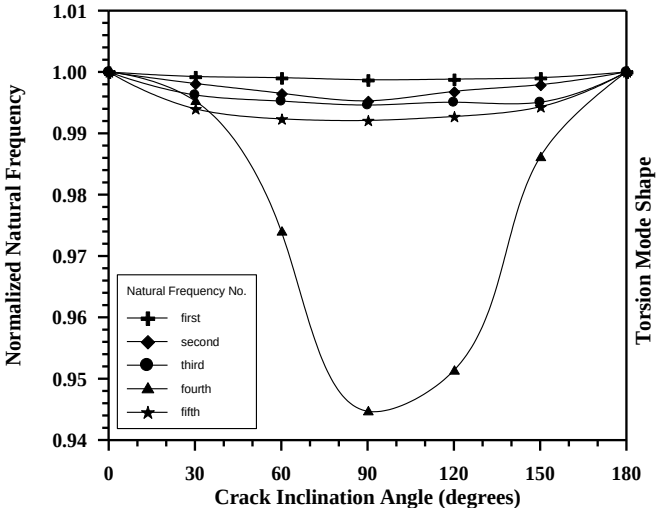

Fig (9): Normalized natural frequency at different crack inclination angles.

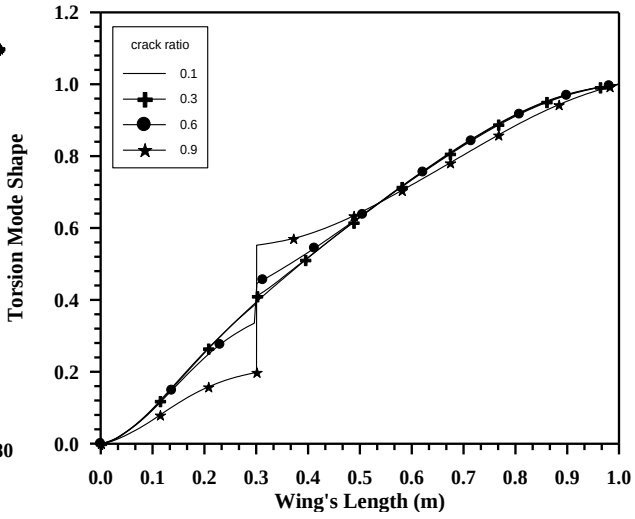

Fig (10): Tensional mode shape at different crack ratios, ζ=0.3.

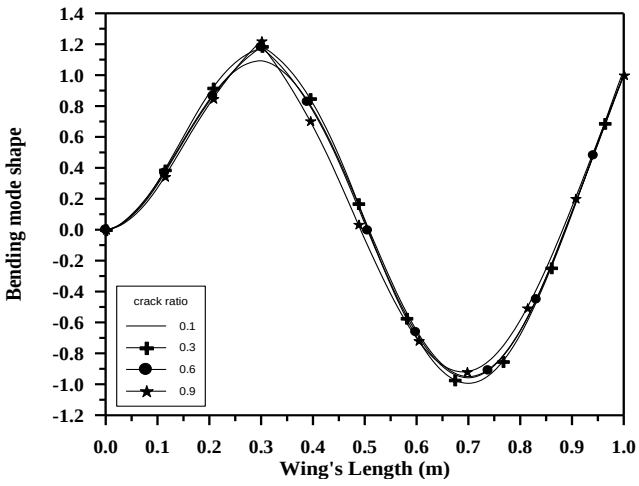

Fig (11): Bending mode shape at different crack ratios, ζ=0.3.

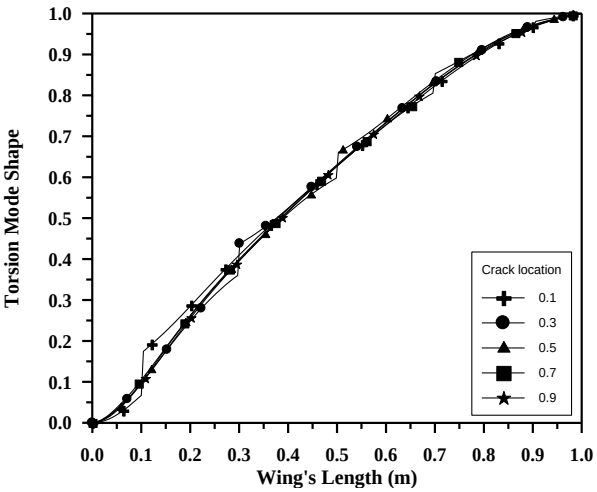

Fig (12): Torsional mode shape at different crack locations, η =0.5.

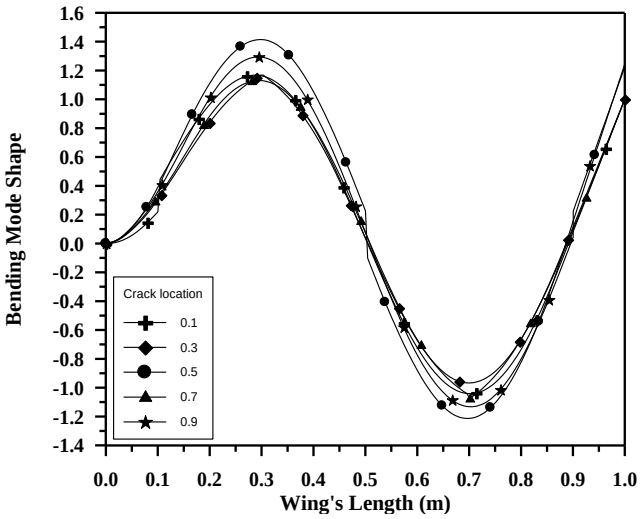

Fig (13): Bending mode shape at different crack locations, η =0.5.

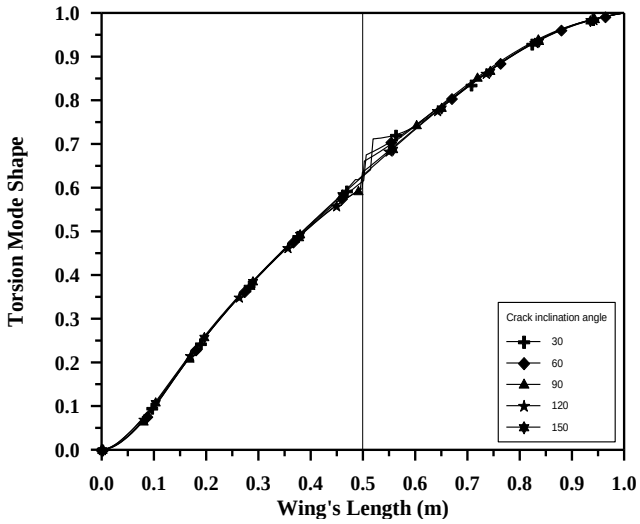

Fig (14): Torsional mode shape at different crack inclination angles.

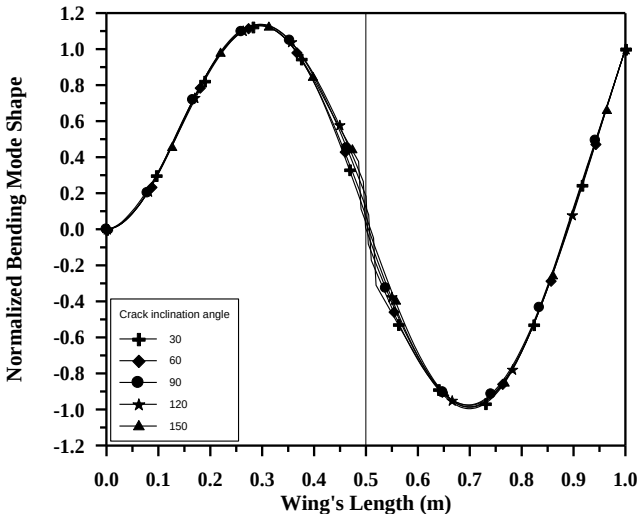

Fig (15): Bending mode shape at different crack inclination angles.

References :

Adams, R. D., Cawley, P., Pye, C. J. and Stone, B. J., 1978, "A vibration technique for non-destructively assessing the integrity of structures," *Journal of Mechanical Engineering Science*, **20**(2), 93-100.

Allemang, R. J., 2002, "The modal assurance criterion (MAC): twenty years of use and abuse," *Proceedings of SPIE*, v. 4753, pp. 397-405.

Cattarius, J. and Inman, D. J., 1997, "Time domain analysis for damage detection in smart structures," *Mechanical Systems and Signal Processing*, **11**(3), 409-423.

Carneiro, S. H. S. and Inman, D. J., 2000, "Continuous mathematical model of cracked Timoshenko beams for damage detection," *Proceeding of the 18th International Modal Analysis Conference*, San Antonio, TX, pp. 194-200.

Cawley, P. and Adams, R. D., 1979, "The location of defects in structures from measurements of natural frequencies," *Journal of Strain Analysis*, **14**(2), 49-57.

Chondros ,T. G., Dimarogonas ,A. D., , and J. Yao, 1998, "A continuous cracked beam vibration theory" *Journal of Sound and Vibration* **215**(1), 17-34.

Cawley, P. and Adams, R. D., 1979, "The location of defects in structures from measurements of natural frequencies," *Journal of Strain Analysis*, **14**(2), 49-57.

Doebling, S. W., Farrar, C. R. and Prime, M. B., 1998, "A summary review of vibration-based damage identification methods," *The Shock and Vibration Digest*, **30**(2), 91-105.

Khan, A. Z., Stanbridge, A. B. and Ewins, D. J., 1999, "Detecting damage in vibrating structures with a scanning LDV," *Optics and Lasers in Engineering*, **32**(6), 583-592.

Lew, J.-S., Sathananthan, S. and Gu, Y., 1997, "Comparison of damage detection algorithms using time domain data," *Proceeding of the 15th International Modal Analysis Conference*, Orlando, FL, pp. 645-651.

Lieven, N. A. J. and Ewins, D. J., 1988, "Spatial correlation of mode shapes, the coordinate modal assurance criterion (COMAC)," *Proceeding of the 6th International Modal Analysis Conference*, Kissimmee, FL, pp. 690-695.

Modena, C., Sonda, D. and Zonta, D., 1999, "Damage localization in reinforced concrete structures by using damping measurements," *Mechanical and Corrosion Properties*, A – Key Engineering Materials, **167**, 132-141.

Natke, H. G. and Cempel, C., 1997, "Model-aided diagnosis based on symptoms," *Proceeding of DAMAS '97, Structural Damage Assessment Using Advanced Signal Processing Procedures*, University of Sheffield, UK, pp. 363-375.

Pandey, A. K., Biswas, M. and Samman, M. M., 1991, "Damage detection from changes in curvature mode shapes," *Journal of Sound and Vibration*, **145**(2), 321-332.

Ratcliffe, C. P., 1997, "Damage detection using a modified Laplacian operator on mode shape data," *Journal of Sound and Vibration*, **204**(3), 505-517.

Stubbs, N. and Osegueda, R., 1990a, "Global non-destructive damage evaluation in solids," *Modal Analysis: the International Journal of Analytical and Experimental Modal Analysis*, **5**(2), 67-79.

Stubbs, N. and Osegueda, R., 1990b, "Global damage detection in solids – experimental verification," *Modal Analysis: the International Journal of Analytical and Experimental Modal Analysis*, **5**(2), 81-97.

Salawu, O. S., 1997, "Detection of structural damage through changes in frequencies: a review," *Engineering Structures*, **19**(9), 718-723.

Shi, Z. Y., Law, S. S. and Zhang, L. M., 2000, "Damage localization by directly using incomplete mode shapes," *Journal of Engineering Mechanics – ASCE*, **126**(6), 656-660.

Van Den Abeele, K. E-A., Sutin, A. Carmeliet, J. and Johnson, P. A., 2001, "Microdamage diagnostics using nonlinear elastic wave spectroscopy (NEWS)," *NDT &E International*, **34**(4), 239-248.

Waheed. S. O, 2006" Dynamic Analysis of Fiber Reinforced Composite Wing under Action of Impulsive excitation", M.sc. Thesis, University of Babylon, Hilla, Iraq.

Wang, K., 2004" Vibration Analysis of Cracked Composite Bending-torsion Beams for Damage Diagnosis"Ph.D., Thesis, Virginia Polytechnic Institute and State University, Virginia, U.S.A.

West, W. M., 1984, "Illustration of the use of modal assurance criterion to detect structural changes in an orbiter test specimen," *Proceedings of the Air Force Conference on Aircraft Structural Integrity*, pp. 1-6.

Yuen, M. M. F., 1985, "A numerical study of the eigenparameters of a damaged cantilever," *Journal of Sound and Vibration*, **103**(3), 301-310.

Zimmerman, D. C. and Kaouk, M., 1994, "Structural damage detection using minimum rank update theory," *Journal of Vibration and Acoustics*, **116**, 222-230.

Zienkiewicz O.C., Taylor R.L.,2000, Vol. 2. The finite element method. Solid mechanics .

ANSYS®, Engineering Analysis System Theoretical Manual, "Http:\\ www. Ansys. Com", Ansys Version 9.0, 2004.